ELSEVIER

Journal of Alloys and Compounds 452 (2008) 467–472

Journal of ALLOYS AND COMPOUNDS

www.elsevier.com/locate/jallcom

Ferroelectric properties of mixed bismuth layer-structured $Na_{0.5}Bi_{8.5}Ti_7O_{27}$ ceramic and $Sr_xNa_{0.5-x/2}Bi_{8.5-x/2}Ti_7O_{27}$ solid solutions

Atsushi Yokoi, Junji Sugishita *

Faculty of Science and Technology, Meijo University, 1-501 Shiogamaguchi, Tempaku-ku, Nagoya 468-8502, Japan

Received 18 May 2007; received in revised form 23 August 2007; accepted 23 August 2007
Available online 28 August 2007

Abstract

Mixed bismuth layer-structured $Na_{0.5}Bi_{8.5}Ti_7O_{27}$ ceramic and $Sr_xNa_{0.5-x/2}Bi_{8.5-x/2}Ti_7O_{27}$ solid solutions were prepared by the solid-state reaction method and the ferroelectric properties of the samples were characterized in this study. As for the $Na_{0.5}Bi_{8.5}Ti_7O_{27}$ ceramic, a single phase (orthorhombic crystal structure with *B*2*cb* space group) was produced at the sintering temperature of 1150 °C. The maximum remanent polarization (P_r) of the $Na_{0.5}Bi_{8.5}Ti_7O_{27}$ ceramic was obtained at the sintering temperature of 1150 °C. On the other hand, the coercive field (E_c) of the sample sintered at 1050 °C for 2 h in air was approximately 100 kV/cm, whereas the values of the samples remained unaltered at the sintering temperatures higher than 1075 °C. From these results, the bulk densities of the samples were connected with the P_r values, because it was recognized that the variations in the bulk density of the samples showed the same tendency as that of the P_r values caused by the increase in the sintering temperature. Also, the Sr substitution for Na and Bi is effective in improving the P_r values of $Sr_xNa_{0.5-x/2}Bi_{8.5-x/2}Ti_7O_{27}$ solid solutions. The Curie temperatures (T_c) of the solid solutions decreased slightly, depending on the composition x, and then the variations in the T_c values are related to the structural distortion caused by the Sr substitution for Na and Bi.

Keywords: Ferroelectric properties; Dielectric properties; $Na_{0.5}Bi_{8.5}Ti_7O_{27}$; X-ray powder diffraction; Solid-state reaction method

1. Introduction

The bismuth layer-structured ferroelectrics (BLSFs) are attractive candidates for use in commercial applications such as the ferroelectric random access memory (FE-RAM). A large remanent polarization (P_r), a low coercive field (E_c) and a high Curie temperature (T_c) are generally required for these applications. In the BLSF compounds, the general formula is indicated by $(Bi_2O_2)^{2+}(A_{m-1}B_mO_{3m+1})^{2-}$, where A is a combination of ions with 12-fold coordination (e.g., Bi, Na and Sr), and B is a combination of ions suitable for 6-fold coordination (e.g., Ti and Nb) [1]. In general, the pseudo-perovskite blocks ($A_{m-1}B_mO_{3m+1}$) are sandwiched between the Bi_2O_2 layers, and these perovskite blocks are composed of m layers of oxygen octahedra with A-site cations. The $(Bi_2O_2)^{2+}$ layers act as the insulating paraelectric layers and considerably affect the electronic response such as the electrical conductivity, band gap, etc., while the ferroelectricity results mainly in the pseudo-perovskite blocks [2]. Furthermore, the spontaneous ferroelectric (P_s) and insulating properties strongly depend on m of the perovskite blocks [3]. Also, BLSF compounds have generally some drawbacks: a relatively low remanent polarization and a high processing temperature [4]; thereby, the improvement of these drawbacks is necessary for their use in commercial applications.

In research field of ferroelectric materials, there is an increasing demand to develop the alternative Pb-free ferroelectric materials to replace the $Pb(Zr_{1-x}Ti_x)O_3$ compounds [5]. Therefore, the BLSF compounds as mentioned above are considered to be one of the appropriate candidates as the Pb-free ferroelectric materials.

The $Na_{0.5}Bi_{8.5}Ti_7O_{27}$ ceramic is one of the complex layered bismuth compounds, where the crystal structure is presented by $Bi_4A_{2m-1}B_{2m+1}O_{6m+9}$ with $m = 3$ and 4. The crystal structure of this compound is a regular intergrowth of $Bi_4Ti_3O_{12}$ ($m = 3$) and $Na_{0.5}Bi_{4.5}Ti_4O_{15}$ ($m = 4$) layers along c-axis [1]. The dielectric and ferroelectric properties of $MBi_8Ti_7O_{27}$ (M = Ca, Sr, Ba and Pb) ceramics have been reported [6–8], however, the ferroelectric properties of $Na_{0.5}Bi_{8.5}Nb_7O_{27}$ ceramic have not been clarified to date. Thus, in order to reveal

* Corresponding author.
E-mail address: sugisita@ccmfs.meijo-u.ac.jp (J. Sugishita).

0925-8388/$ – see front matter © 2007 Elsevier B.V. All rights reserved.
doi:10.1016/j.jallcom.2007.08.056

the ferroelectric properties of $Na_{0.5}Bi_{8.5}Ti_7O_{27}$ ceramic, the $Na_{0.5}Bi_{8.5}Ti_7O_{27}$ ceramic was prepared by the solid-state reaction method; the relationship between synthesis and ferroelectric properties of $Na_{0.5}Bi_{8.5}Ti_7O_{27}$ ceramic was investigated in this study. Moreover, the effects of the Sr^{2+} substitution for Na^+ and Bi^{3+} on the dielectric and ferroelectric properties of $Sr_xNa_{0.5-x/2}Bi_{8.5-x/2}Nb_7O_{27}$ solid solutions were also investigated.

2. Experimental method

High-purity (>99.9%) $SrCO_3$, Na_2CO_3, Bi_2O_3 and TiO_2 powders weighed on the basis of their stoichiometric composition were mixed and calcined at 800 °C for 4 h in air. These calcined powders were re-ground and mixed with a polyvinyl alcohol, and then pressed into a pellet of 12 mm in diameter and 3 mm in thickness under the pressure of 100 MPa. Subsequently, the pellet of $Na_{0.5}Bi_{8.5}Ti_7O_{27}$ ceramic and the $Sr_{0.5}Bi_{8.5-x/2}Na_{1.5-x/2}Ti_7O_{27}$ solid solutions were sintered at the various temperatures ranging from 1050 to 1150 °C for 2 h in air. The bulk density of the sintered sample was measured by using Archimedes method. The crystalline phase of the crushed sample was identified by the X-ray powder diffraction (XRPD) with Cu Kα radiation. Also, the lattice parameters of the samples were calculated by using the least squares method [9]. The microstructure of the samples was examined using a field emission scanning microscopy (FE-SEM). In order to evaluate the temperature dependence of dielectric constants, these pellets were electroded by a platinum paste and fired at 850 °C for 30 min. The temperature dependence of the dielectric constant was measured at 1 MHz by a LCR meter in the temperature range from room temperature to 800 °C. The *P–E* hysteresis loop at room temperature was observed using an aixACCT TF2000FE-HV ferroelectric test unit at 50 Hz in silicon oil.

3. Results and discussion

3.1. Synthesis and ferroelectric properties of $Na_{0.5}Bi_{8.5}Ti_7O_{27}$ ceramic

Fig. 1 shows the XRPD patterns of $Na_{0.5}Bi_{8.5}Ti_7O_{27}$ ceramic sintered in the temperature range of 1050–1150 °C for 2 h in air. From the XRPD patterns of $Na_{0.5}Bi_{8.5}Ti_7O_{27}$ ceramic sintered at the various temperatures, the single phase of the $Na_{0.5}Bi_{8.5}Ti_7O_{27}$ ceramic was obtained at the sintering

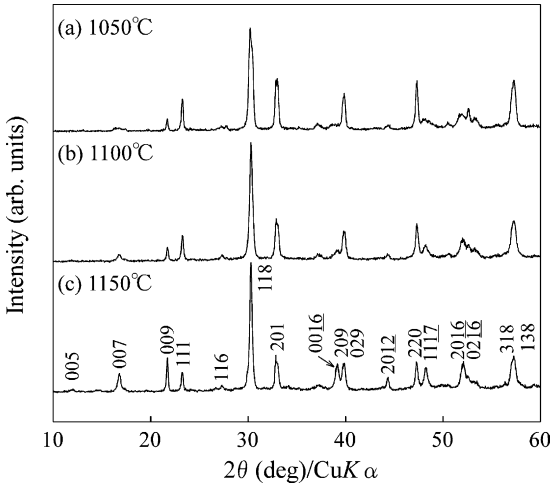

Fig. 1. XRPD patterns of $Na_{0.5}Bi_{8.5}Ti_7O_{27}$ ceramic sintered at various temperatures for 2 h in air.

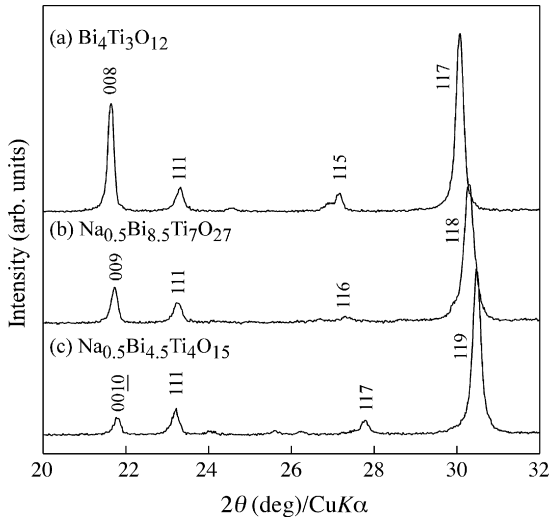

Fig. 2. XRPD patterns of (a) $Bi_4Ti_3O_{12}$, (b) $Na_{0.5}Bi_{8.5}Ti_7O_{27}$ and (c) $Na_{0.5}Bi_{4.5}Ti_4O_{15}$ ceramics sintered at various temperatures for 2 h in air.

temperature of 1150 °C, which is an orthorhombic crystal structure with *B*2*cb* space group [10]. However, the single phase of the $Na_{0.5}Bi_{8.5}Ti_7O_{27}$ ceramic was not recognized at the sintering temperatures smaller than 1100 °C. Fig. 2 gives XRPD patterns of $Bi_4Ti_3O_{12}$, $Na_{0.5}Bi_{8.5}Ti_7O_{27}$ and $Na_{0.5}Bi_{4.5}Ti_4O_{15}$ ceramics sintered at the various temperatures. The $(h\,k\,l)$ peak of the $Na_{0.5}Bi_{8.5}Ti_7O_{27}$ located at the middle of the $(h\,k\,l-1)$ peak of $Bi_4Ti_3O_{12}$ and the $(h\,k\,l+1)$ peak of $Na_{0.5}Bi_{4.5}Ti_4O_{15}$. Similar results have been demonstrated previously for $Bi_4Ti_3O_{12}$–$SrBi_4Ti_4O_{15}$ compounds [11]. For instance, the 2θ for peak (1 1 5) of $Bi_4Ti_3O_{12}$ ceramic is 27.18°, the 2θ for peak (1 1 7) of $Na_{0.5}Bi_{4.5}Ti_4O_{15}$ ceramic is 27.78° and the peak (1 1 6) of $Na_{0.5}Bi_{8.5}Ti_7O_{27}$ ceramic locates at 27.30°.

As mentioned previously, the crystal structure of $Na_{0.5}Bi_{8.5}Ti_7O_{27}$ ceramic consists of the structural units of two parent phases such as $Bi_4Ti_3O_{12}$ ($m=3$) and $Na_{0.5}Bi_{4.5}Ti_4O_{15}$ ($m=4$) compounds by sharing the 'Bi_2O_2' sheets along the *c*-axis as shown in Fig. 3.

Moreover, the bulk densities of the samples as a function of sintering temperature are shown in Fig. 4. The bulk densities of the samples were drastically increased from 5.89 to 7.17 g/cm^3 in the sintering temperature range of 1050–1100 °C, while the values of the samples remained the constant value at the sintering temperatures above 1100 °C. Thus, it was found that the increase in the sintering temperature was effective in improving the bulk density of the samples.

In order to elucidate the increase in the bulk density caused by the increasing the sintering temperature, the morphological changes in the samples were investigated by using the FE-SEM. Fig. 5 gives the morphological changes in the samples sintered at 1075 and 1100 °C for 2 h in air. When comparing these photographs, the reduction of porosity and the grain growth was observed and these results agreed with the increase in the bulk density as described above. Therefore, an increase in the sintering temperature leads to increased densification, as would be expected. In order to see whether the ferroelectric properties were also affected, the hysteresis loops of the samples sin-

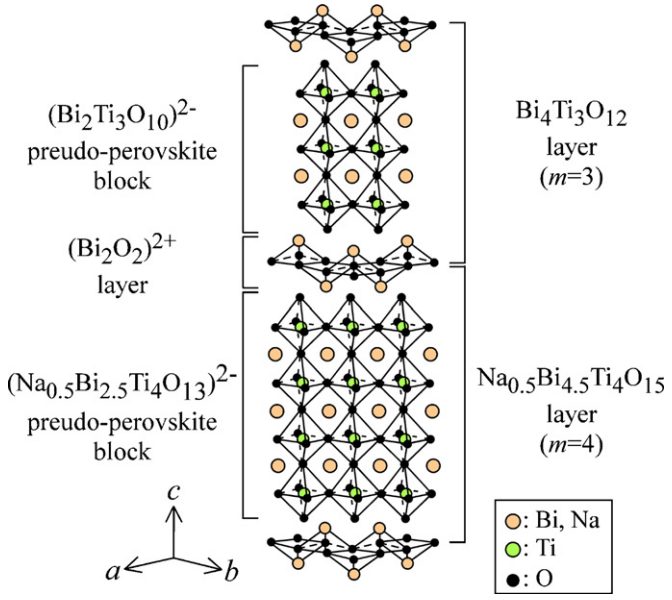

Fig. 3. Schematic diagram of crystal structure of $Na_{0.5}Bi_{8.5}Ti_7O_{27}$ ceramic.

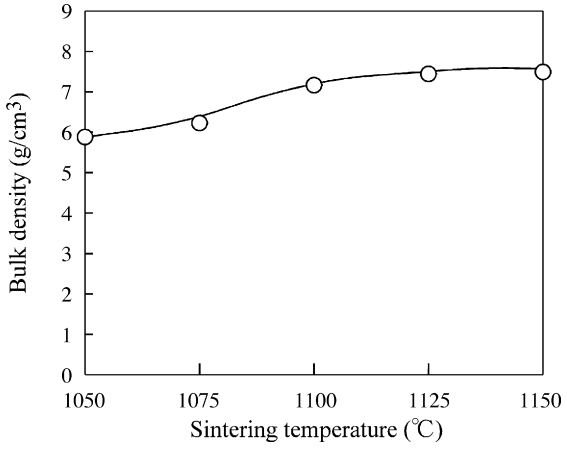

Fig. 4. Variations in bulk density of $Na_{0.5}Bi_{8.5}Ti_7O_{27}$ ceramic sintered at various temperatures for 2 h in air.

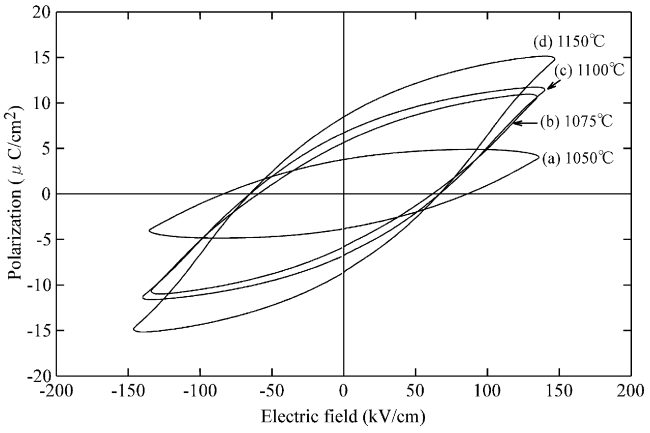

Fig. 6. *P–E* hysteresis loops of $Na_{0.5}Bi_{8.5}Ti_7O_{27}$ ceramic sintered at various temperatures for 2 h in air.

tered at various temperatures were observed, using an aixACCT TF2000FE-HV ferroelectric test unit.

Fig. 6 shows the *P–E* hysteresis loops of the $Na_{0.5}Bi_{8.5}Ti_7O_{27}$ ceramic measured at room temperature. The increase in the sintering temperature was effective in improving the P_r value of the ceramic. The P_r values of the ceramic increased from 4 to 9 μC/cm^2 with increasing the sintering temperature, whereas the E_c values of the ceramic remained constant at approximately 65 kV/cm in the sintering temperature range of 1075–1150 °C. From these results, the substitution for the other element in the ceramic is necessary in order to improve the P_r and E_c values.

The temperature dependence of dielectric constant of the $Na_{0.5}Bi_{8.5}Ti_7O_{27}$ ceramic is shown in Fig. 7. As for the $Na_{0.5}Bi_{8.5}Ti_7O_{27}$ ceramic, two peaks are present at the temperature of approximately 662 and 673 °C, respectively. A similar result was also reported in the mixed bismuth layer-structured $Bi_7Ti_4NbO_{21}$ ceramic [12] and the former is attributed to a phase transition within the orthorhombic crystal structure by a space group change and the latter corresponds to the Curie temperature (T_c) [13]. Thus, these peaks were related to the Curie temperatures of the $Bi_4Ti_3O_{12}$ and $Na_{0.5}Bi_{4.5}Ti_4O_{15}$ ceramics, because

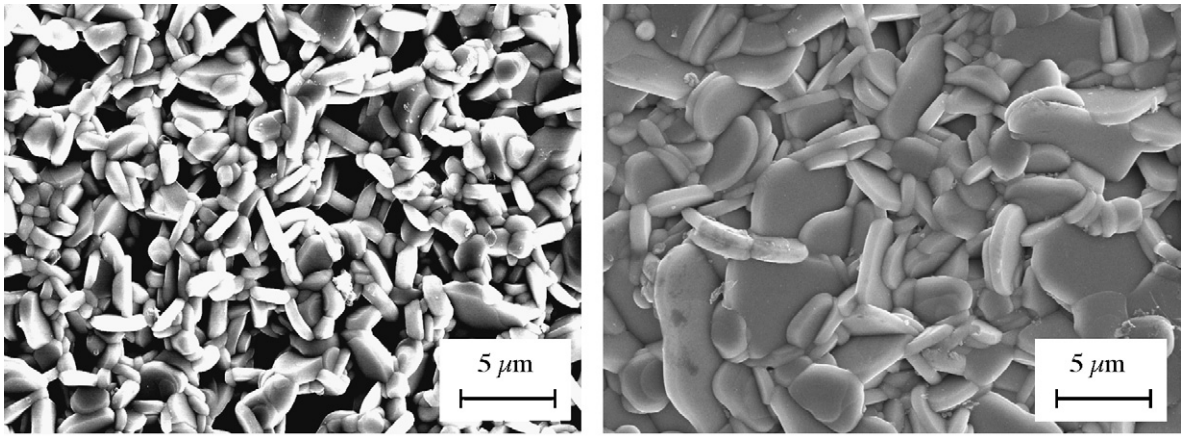

(a) 1075℃ (b) 1100℃

Fig. 5. FE-SEM photographs of $Na_{0.5}Bi_{8.5}Ti_7O_{27}$ ceramic sintered at 1075 and 1100 °C for 2 h in air.

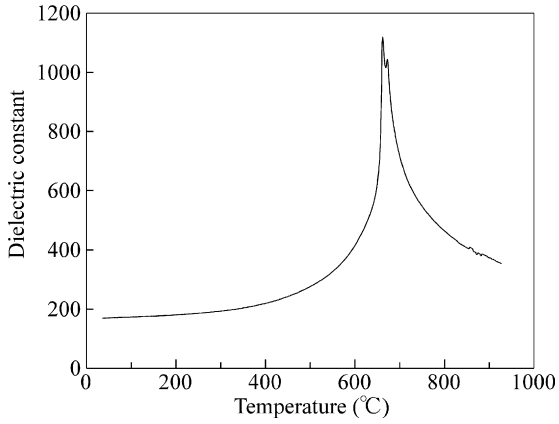

Fig. 7. Temperature dependence of dielectric constant of $Na_{0.5}Bi_{8.5}Ti_7O_{27}$ ceramic measured at a frequency of 1 MHz.

the Curie temperatures of the $Bi_4Ti_3O_{12}$ and $Na_{0.5}Bi_{4.5}Ti_4O_{15}$ ceramics are 675 and 650 °C, respectively [14,15].

3.2. Crystal structure and ferroelectric properties of $Sr_xNa_{0.5-x/2}Bi_{8.5-x/2}Ti_7O_{27}$ solid solutions

In general, it is known that the Sr substitution for Na and Bi is effective in improving the ferroelectric properties of BLSF compounds [16]. Thus, in order to improve the ferroelectric properties of $Na_{0.5}Bi_{8.5}Ti_7O_{27}$ ceramic, the Sr substitution for Na and Bi was performed and the $Sr_xNa_{0.5-x/2}Bi_{8.5-x/2}Ti_7O_{27}$ solid solutions were synthesized in this study. Fig. 8 shows the XRPD patterns of $Sr_xNa_{0.5-x/2}Bi_{8.5-x/2}Ti_7O_{27}$ solid solutions sintered at various temperatures for 2 h in air. From the XRPD results, no secondary phase was detected over the whole composition range; XRPD patterns for these samples in which all peaks can be indexed in the correct space group *B*2*cb* as described earlier. Moreover, the peak shifts to a low angular of 2θ were recognized with increasing the composition *x*. Thus, it is expected that the lattice parameters are varied by the Sr substitution for

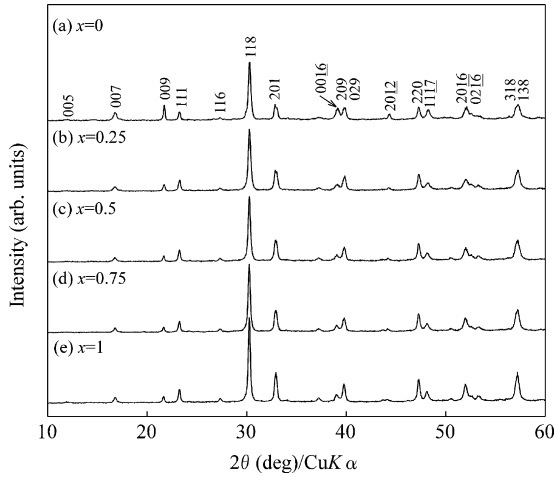

Fig. 8. XRPD patterns of $Sr_xNa_{0.5-x/2}Bi_{8.5-x/2}Ti_7O_{27}$ solid solutions sintered at various temperatures for 2 h in air.

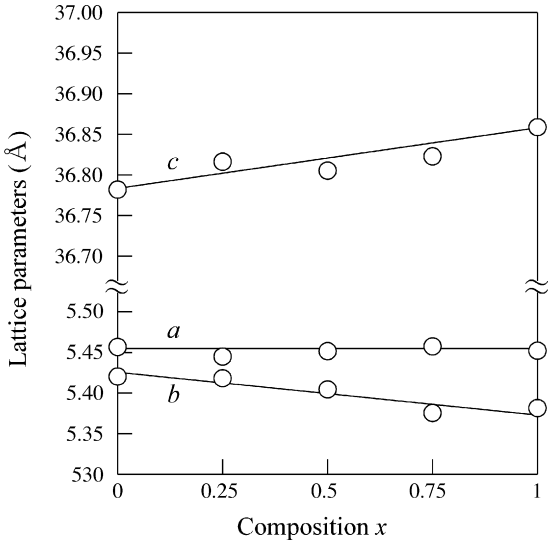

Fig. 9. Effects of Sr substitution for Na and Bi on lattice parameters of $Sr_xNa_{0.5-x/2}Bi_{8.5-x/2}Ti_7O_{27}$ solid solutions.

Na and Bi; the lattice parameters of the samples are calculated in terms of the least squares method, and are shown in Fig. 9. All the lattice parameters varied linearly, depending on the composition *x*; therefore, these results are predominantly due to the ionic radii, because the ionic radius of Sr^{2+} (1.44 Å) is larger than the ionic radii of Na^+ (1.39 Å) and Bi^{3+} (1.3 Å), when the coordination number is twelve [14,17]. From these results, it was considered that the $Sr_xNa_{0.5-x/2}Bi_{8.5-x/2}Ti_7O_{27}$ solid solutions satisfied Vegard's law, because of the linearly variations in the lattice parameters of the solid solutions that were shown in the composition range of 0–1.

Fig. 10 gives the *P*–*E* hysteresis loops of the $Sr_xNa_{0.5-x/2}Bi_{8.5-x/2}Ti_7O_{27}$ solid solutions sintered at various temperatures for 2 h in air. The Sr substitution for Na and Bi was effective in improving the P_r values. Fig. 11 gives the P_r and E_c values of the solid solutions caused by the Sr substitution for Na and Bi. The P_r values of the solid solutions linearly increased from 9 to 11 μC/cm^2 with increasing the composition *x*. On the other hand, the E_c values of the samples increased, depending on the composition *x*, and then the additional modification

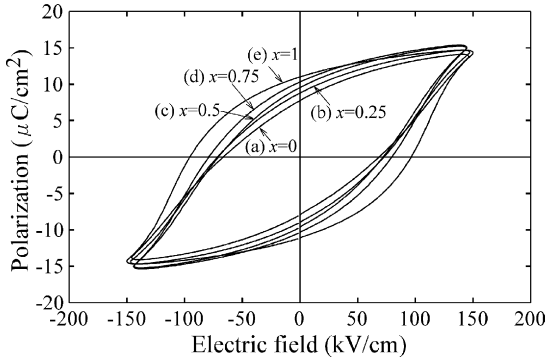

Fig. 10. *P*–*E* hysteresis loops of $Sr_xNa_{0.5-x/2}Bi_{8.5-x/2}Ti_7O_{27}$ solid solutions obtained at room temperature.

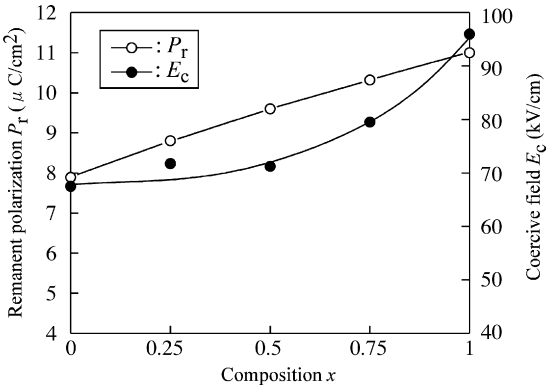

Fig. 11. Effects of Sr substitution for Na and Bi on (a) remanent ferroelectric and (b) coercive field of $Sr_xNa_{0.5-x/2}Bi_{8.5-x/2}Ti_7O_{27}$ solid solutions.

in E_c values is required for the commercial applications. A similar result was also recognized in the P_r and E_c values of $SrBi_8Ti_7O_{27}$ ceramic as reported by Noguchi et al. [8].

The temperature dependence of the dielectric constant of the $Sr_xNa_{0.5-x/2}Bi_{8.5-x/2}Ti_7O_{27}$ solid solutions measured at a frequency of 1 MHz is shown in Fig. 12. In the case of $Na_{0.5}Bi_{7.5}Ti_7O_{27}$ ceramic, it was found that two peaks present at the temperatures of approximately 662 and 673 °C as mentioned earlier, however, a single peak was recognized with increasing the composition x. The Curie temperature of the $Sr_xNa_{0.5-x/2}Bi_{8.5-x/2}Ti_7O_{27}$ solid solutions linearly decreased, depending on the composition x. Other studies indicate that the Curie temperature of the bismuth layer-structured ferroelectric correlated with structure distortion in the pseudo-perovskite block; therefore, the relationship between the T_c and the structural distortion of the pseudo-perovskite block, i.e., the tolerance factor (t) of the pseudo-perovskite block, was investigated in this study [14,18]. The tolerance factor is determined by the following equation [19]:

$$t = \frac{R_A + R_O}{\sqrt{2}(R_B + R_O)} \quad (1)$$

where R_A, R_B and R_O are the ionic radii of A, B and O ions, respectively. The t values in the pseudo-perovskite block of the

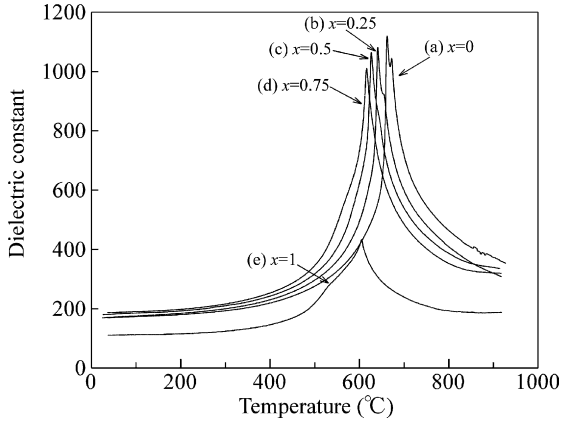

Fig. 12. Temperature dependence of dielectric constant of $Sr_xNa_{0.5-x/2}Bi_{8.5-x/2}Ti_7O_{27}$ solid solutions measured at a frequency of 1 MHz.

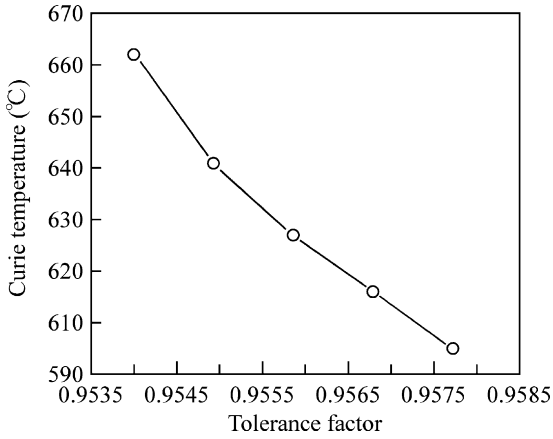

Fig. 13. Relationship between Curie temperature and tolerance factor of $Sr_xNa_{0.5-x/2}Bi_{8.5-x/2}Ti_7O_{27}$ solid solutions.

$Sr_xNa_{0.5-x/2}Bi_{8.5-x/2}Ti_7O_{27}$ solid solutions linearly increased from 0.954 to 0.958 in the composition range of $x = 0$–1. Thus, the relationship between the tolerance factor and the Curie temperature are given in Fig. 13. It was considered that the decrease in T_c is attributed to the increase in the t values, i.e., the increase in the structural distortion of the pseudo-perovskite block caused by the Sr substitution for Na and Bi.

4. Conclusions

$Na_{0.5}Bi_{8.5}Ti_7O_{27}$ ceramic was synthesized, and the relationship between the Sr substitution for Na and Bi and ferroelectric properties of the $Sr_xNa_{0.5-x/2}Bi_{8.5-x/2}Ti_7O_{27}$ solid solutions were investigated in this study.

(1) From the XRPD patterns of $Na_{0.5}Bi_{8.5}Ti_7O_{27}$ ceramic sintered at various temperatures for 2 h in air, the single phase of the sample was obtained at the sintering temperature of 1150 °C, which is an orthorhombic crystal structure with *B2cb* space group as indicated above. The P_r value of the ceramic increased with increasing the sintering temperature; therefore, it was considered that the variations in the bulk densities of the $Na_{0.5}Bi_{8.5}Ti_7O_{27}$ ceramic depended on the P_r values caused by the increase in the sintering temperature. However, the E_c values of the samples were on the order of approximately 65 kV/cm at the sintering temperatures above 1075 °C.

(2) As for the Sr substitution for Na and Bi, the secondary phase was not detected over the whole composition range. The Sr substitution for Na and Bi was effective in improving the P_r values of $Sr_xNa_{0.5-x/2}Bi_{8.5-x/2}Ti_7O_{27}$ solid solutions and the maximum P_r value is 11 μC/cm^2 at $x = 1$. On the other hand, the E_c values of the solid solutions slightly increased from 65 to 95 kV/cm with increasing the composition x; the substitution of the other elements in this sample is necessary in order to improve the E_c values. Furthermore, the decrease in the Curie temperature of the $Sr_xNa_{0.5-x/2}Bi_{8.5-x/2}Ti_7O_{27}$ solid solutions is attributed to the increase in the tolerance factor of the pseudo-perovskite block.

References

[1] S. Mallick, K.J. Bowman, A.H. King, Appl. Phys. Lett. 86 (2005) 182902–182911.
[2] A.D. Rae, J.G. Thompson, R.L. Withers, Acta Crystallogr. B 48 (1992) 418.
[3] T. Kobayashi, Y. Noguchi, M. Miyayama, Jpn. J. Appl. Phys. 43 (2004) 6653.
[4] Y. Wu, G. Cao, J. Mater. Res. 15 (2000) 1583.
[5] K. Kakimoto, I. Masuda, H. Ohsato, J. Eur. Ceram. Soc. 25 (2005) 2719.
[6] R. Maalal, M. Manier, J.P. Mercurio, J. Eur. Ceram. Soc. 15 (1995) 1135.
[7] T. Kikuch, A. Watanabe, K. Uchida, Mater. Res. Bull. 12 (1977) 299.
[8] Y. Noguchi, M. Miyayama, T. Kudo, Appl. Phys. Lett. 77 (2000) 3639.
[9] G. Martínez-Lozano, M. Hesiquio-Garduño, B. Zeifert, J. Salmones, J. Alloys. Compd. 434–435 (2007) 816.
[10] K. Uchida, T. Kikuchi, J. Am. Ceram. Soc. 61 (1978) 5.
[11] J. Zhu, X.-Y. Mao, X.-B. Chen, J. Cryst. Growth 277 (2005) 462.
[12] A. Yokoi, H. Ogawa, Mater. Sci. Eng. B 129 (2006) 80.
[13] R. Maalal, D. Mercurio, G. Trolliard, J.P. Mercurio, Ann. Chim. Sci. Mater. 23 (1998) 247.
[14] D.Y. Suárez, I.M. Reaney, W.E. Lee, J. Mater. Res. 16 (2001) 3139.
[15] C.W. Ahn, W. Kim, M.S. Ha, K. Won, J.S. Lee, S.-S. Yi, Ferroelectric 273 (2002) 261.
[16] A. Yokoi, H. Ogawa, S. Kume, Physica B 389 (2007) 317.
[17] R.D. Shannon, J. Appl. Phys. 73 (1993) 348.
[18] Y. Wu, M.J. Forbess, S. Seraji, S.J. Limmer, T.P. Chou, C. Nguyen, G. Cao, J. Appl. Phys. 90 (2001) 5296.
[19] S.V. Bhide, A.V. Virkar, J. Electrochem. Soc. 146 (1999) 4386.